**Electronic Supplementary Materials (ESI)**

**Supporting information**

# Tuning the Electronic Properties of a Nitro- and Cyano-Functionalized benzothienoquinolizinium Salt as Potential Organic N-Type Semiconductor : Experimental and Theoretical Study

**Andrés Aracena *, Kerry Wrighton-Araneda, Katherine Pezet, Diego Vilches, Felipe A. Angel, Ihan Chandía, César Zúñiga, Sebastián Elgueta and Javiera González.**

## Experimental characterization

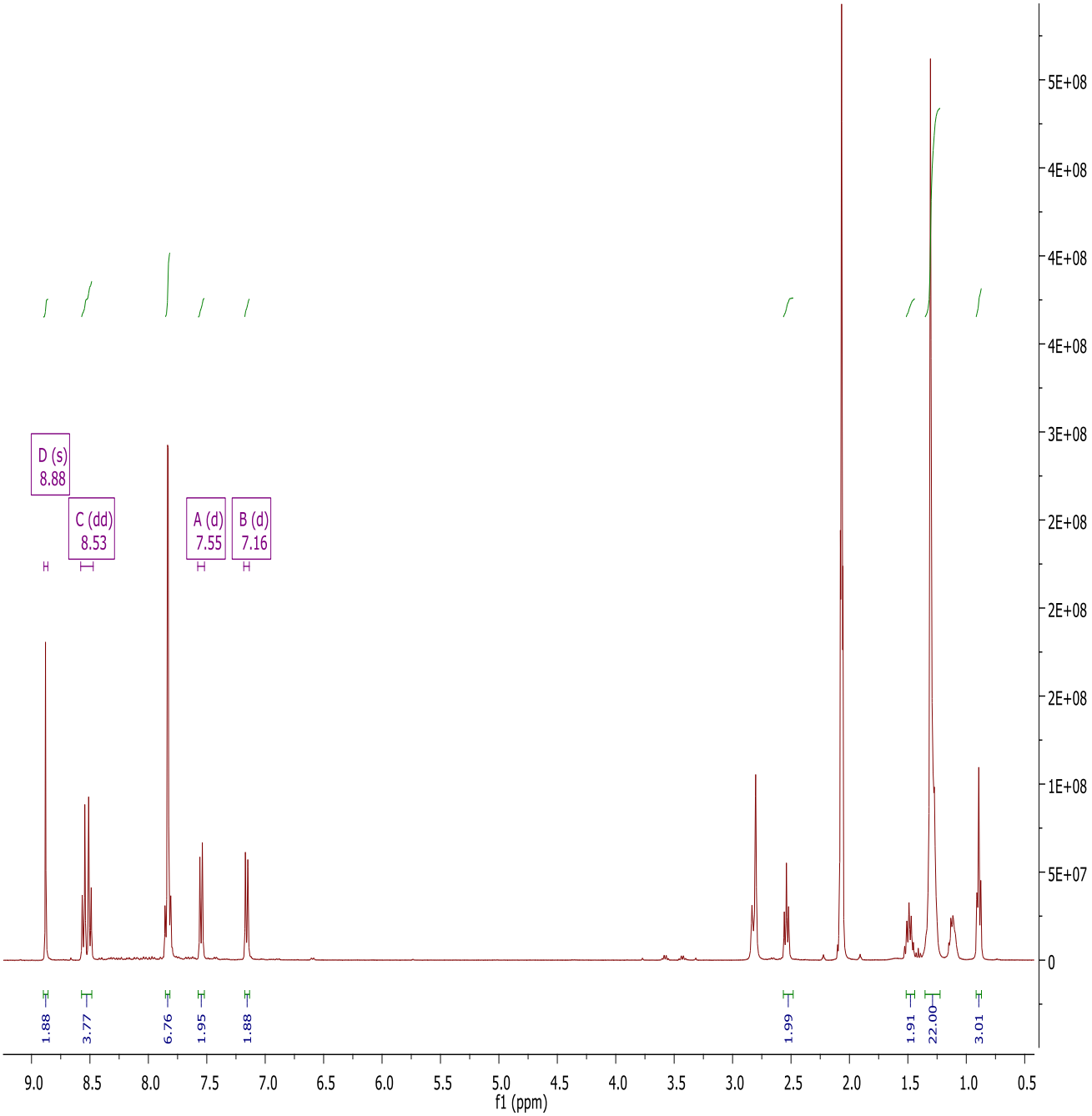



**Figure S1.** $^{1}$H NMR spectrum (400 MHz, acetone-$d_6$) of the pyridinium salt precursor **3**.

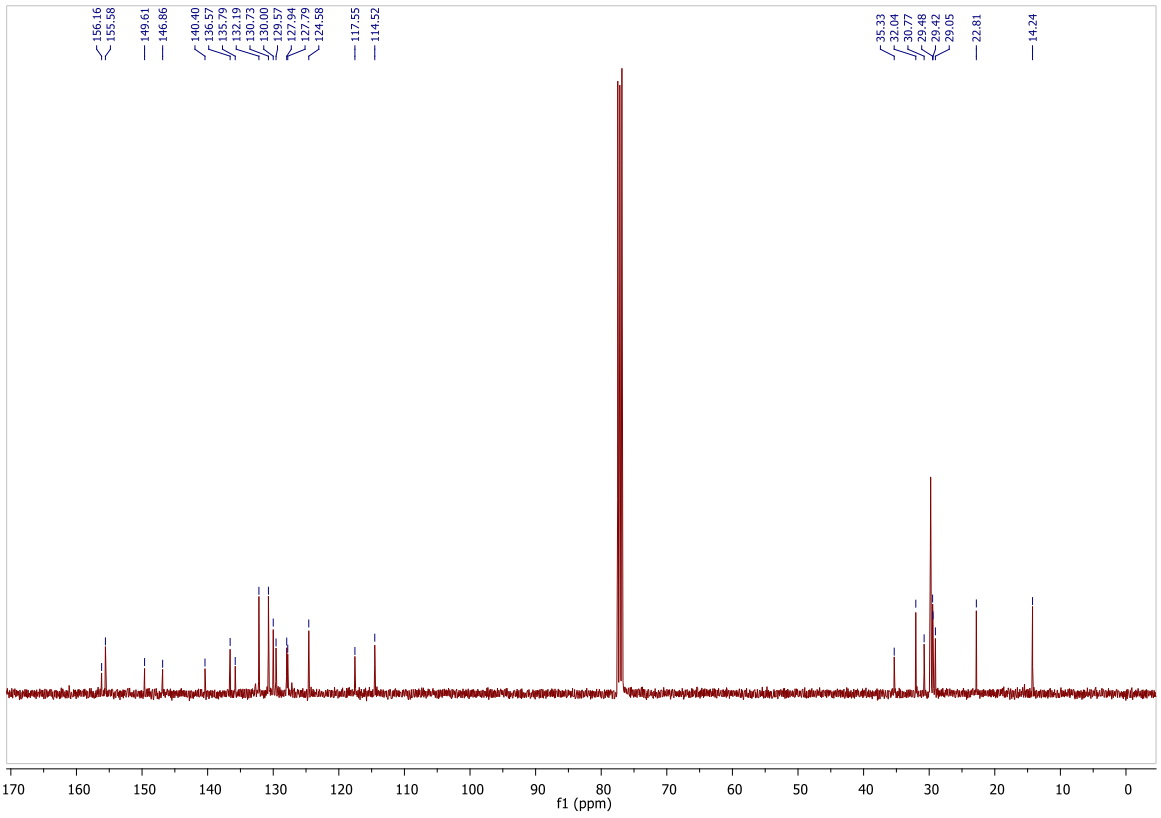



**Figure S2.** $^{13}C$ NMR spectrum (101 MHz, chloroform-*d*) of the pyridinium salt precursor **3**.

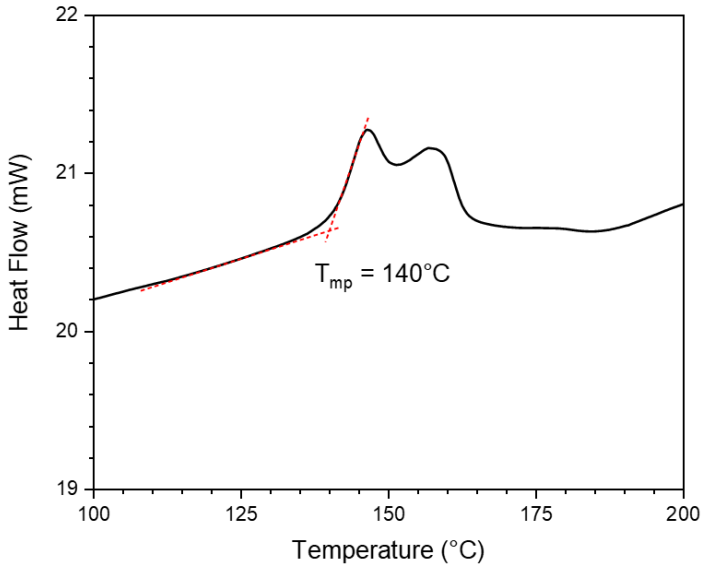



**Figure S3.** DSC thermogram of compound **3**, showing an endothermic melting transition with an onset temperature of 140 °C.

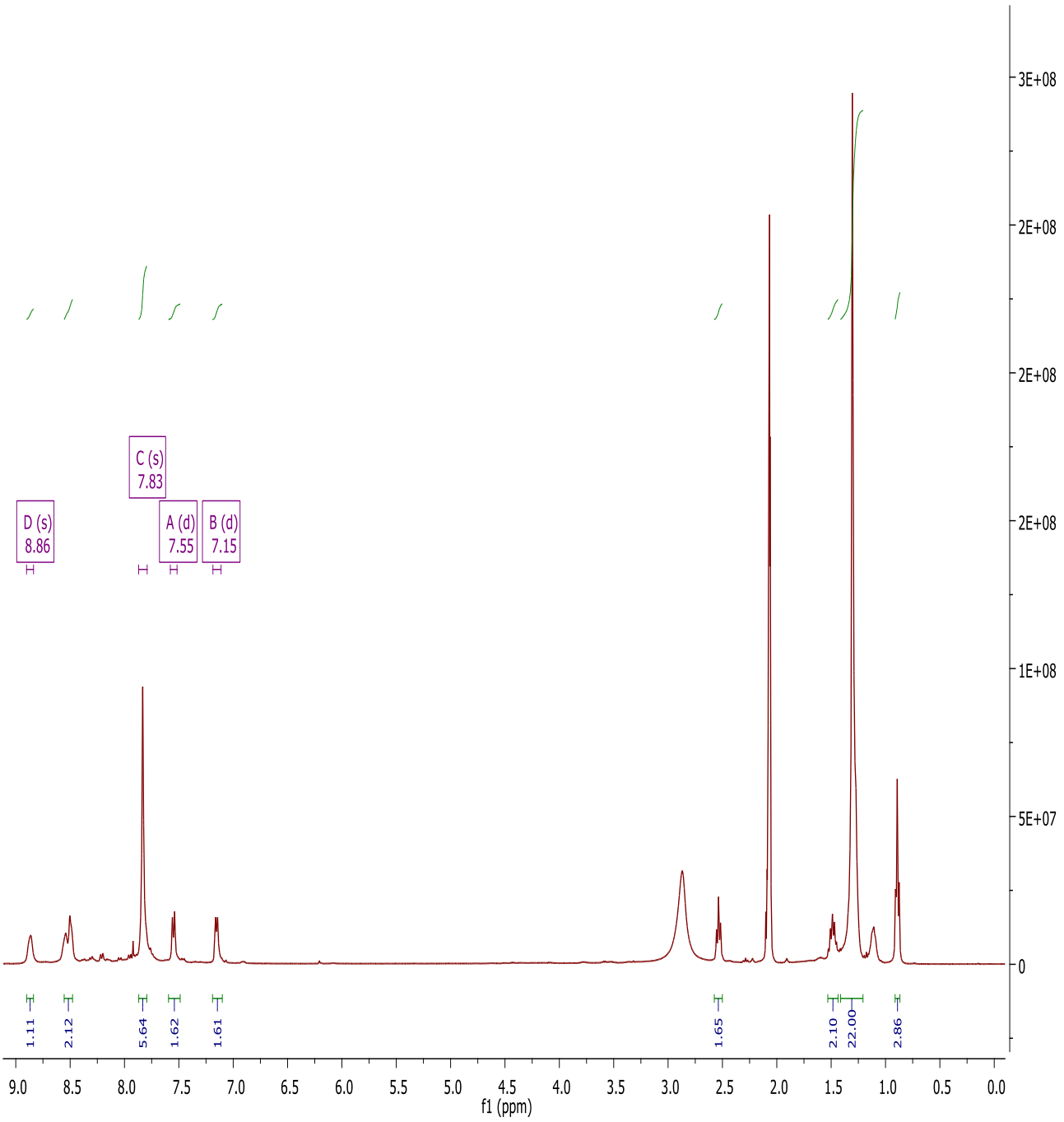



**Figure S4.** $^{1}$H NMR spectrum (400 MHz, acetone-$d_6$) of the photocyclised benzothienoquinolizinium tetrafluoroborate **4**.

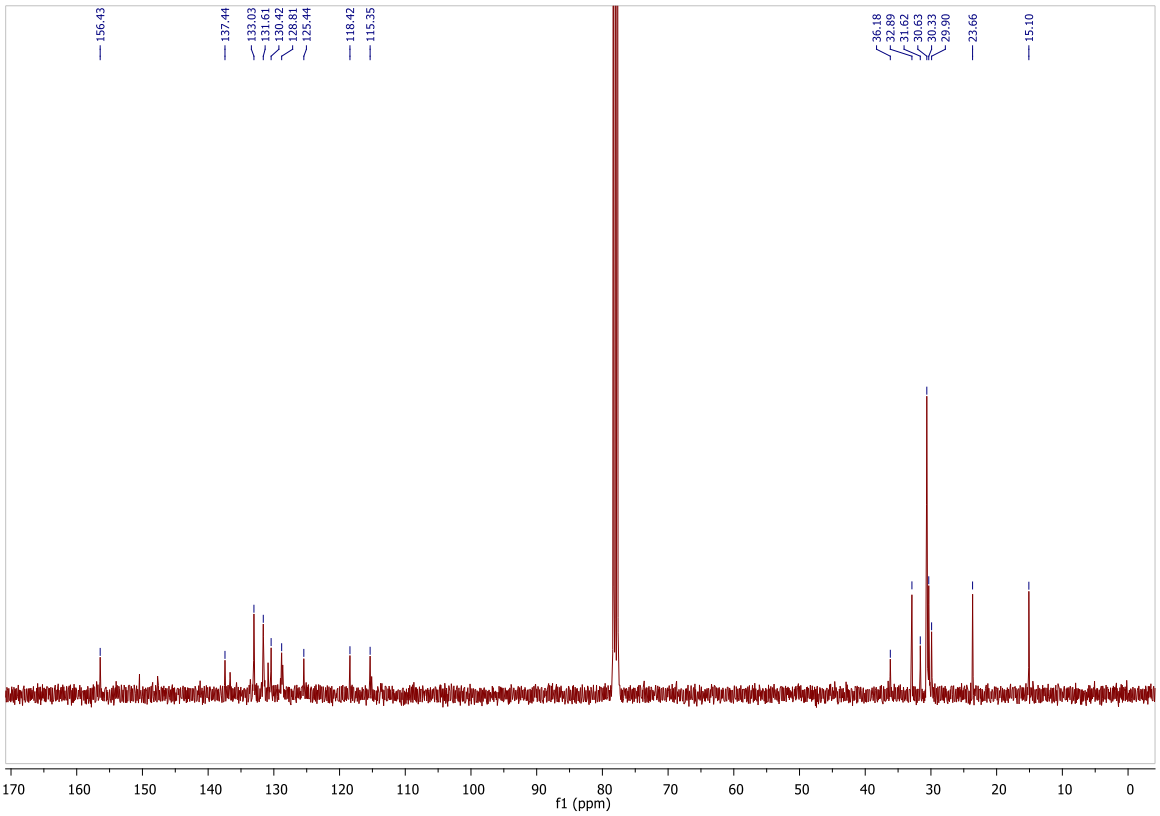



**Figure S5.** $^{13}C$ NMR spectrum (101 MHz, chloroform-*d*) of the photocyclised benzothienoquinolizinium tetrafluoroborate **4**.

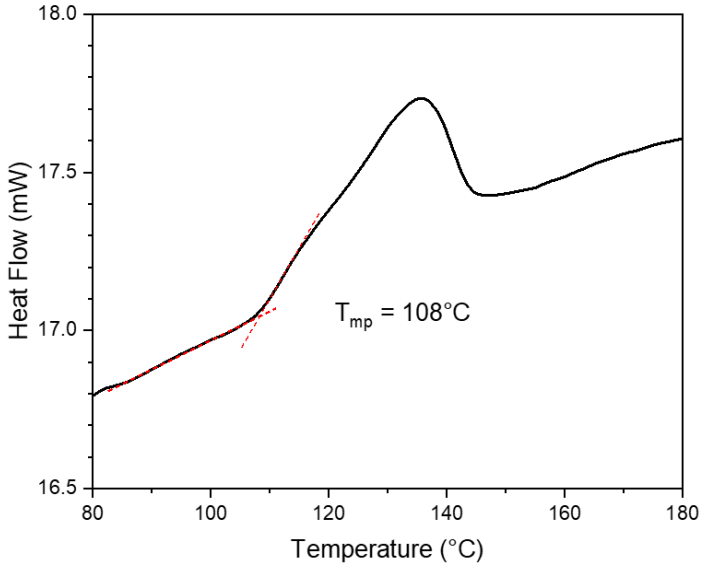



**Figure S6.** DSC thermogram of compound **4**, showing an endothermic melting transition with an onset temperature of 108 °C.

**Electrochemical characterization**

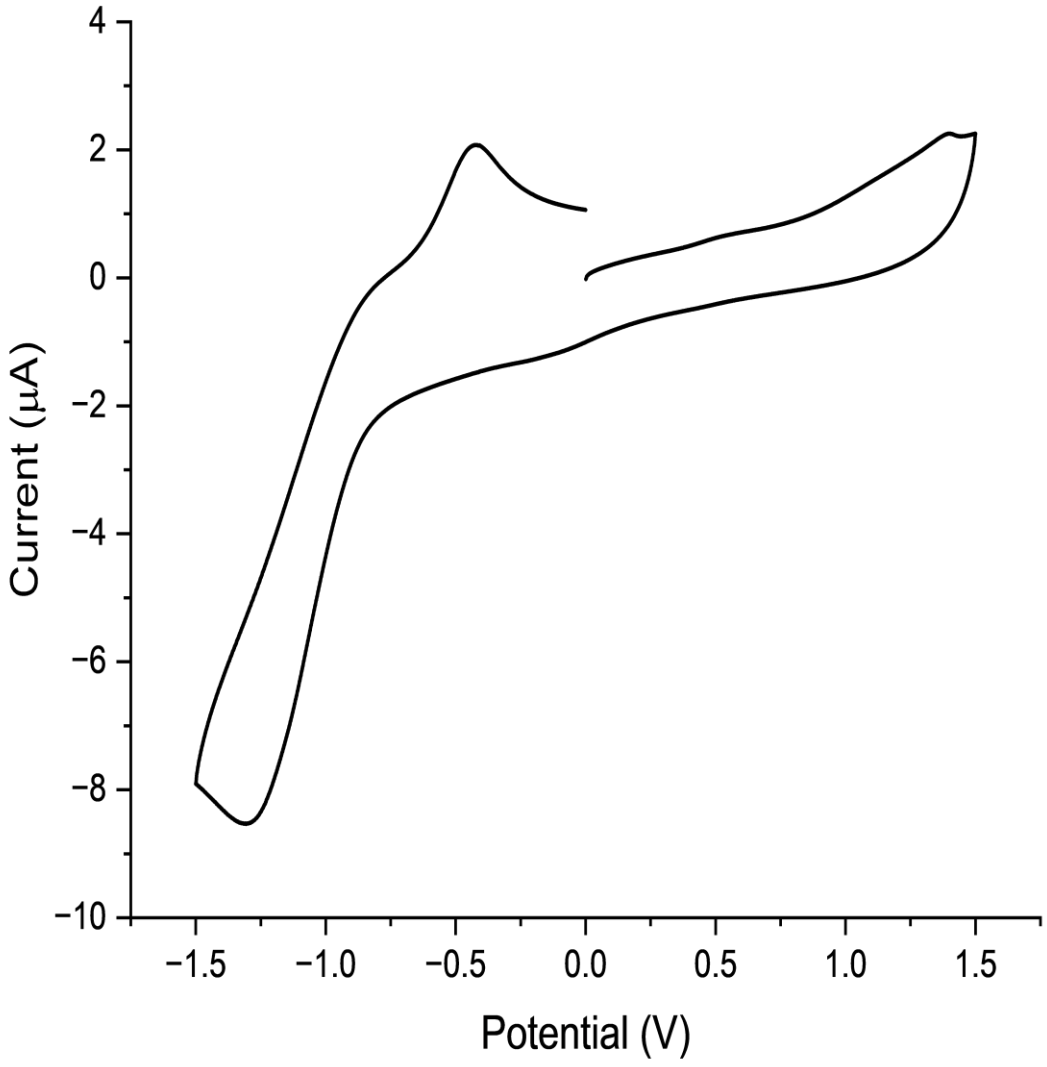



**Figure S7.** Cyclic voltammogram of the blank supporting-electrolyte solution containing 0.1 M $Bu_4NPF_6$ in anhydrous acetonitrile, recorded under nitrogen at a scan rate of 50 mV $s^{-1}$.

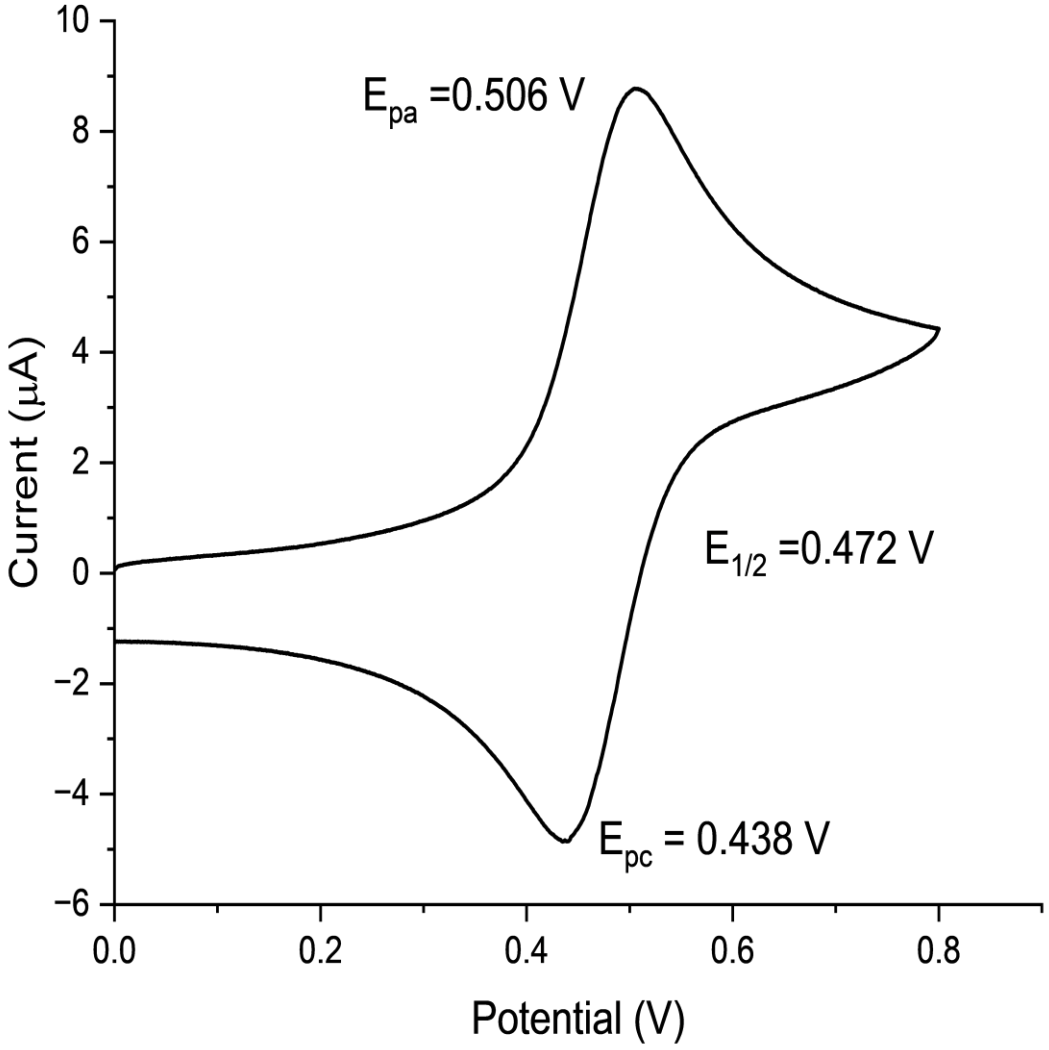



**Figure S8.** Cyclic voltammogram of the ferrocene/ferrocenium ($Fc/Fc^+$) redox couple in anhydrous acetonitrile containing 0.1 M $Bu_4NPF_6$, recorded under nitrogen at a scan rate of 50 mV $s^{-1}$. The half-wave potential was determined as $E_{1/2}$ = 0.472V vs. Ag/AgCl.

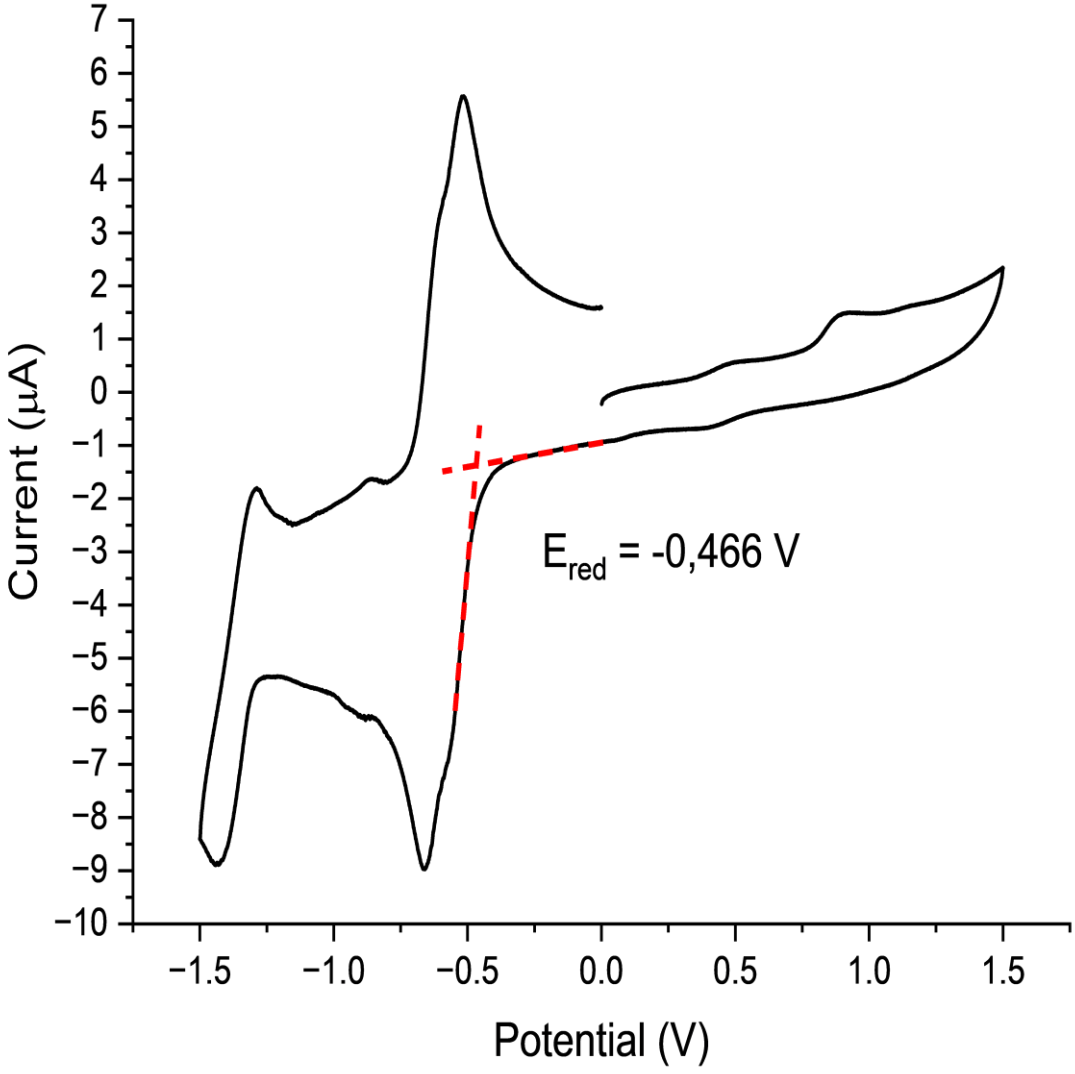



**Figure S9:** Cyclic voltammogram of the pyridinium salt precursor **3** in anhydrous acetonitrile containing 0.1 M $Bu_4NPF_6$, recorded under nitrogen at a scan rate of 50 mV $s^{-1}$. The reduction potential was determined as $E_{red} = -0.466V$ vs. Ag/AgCl.

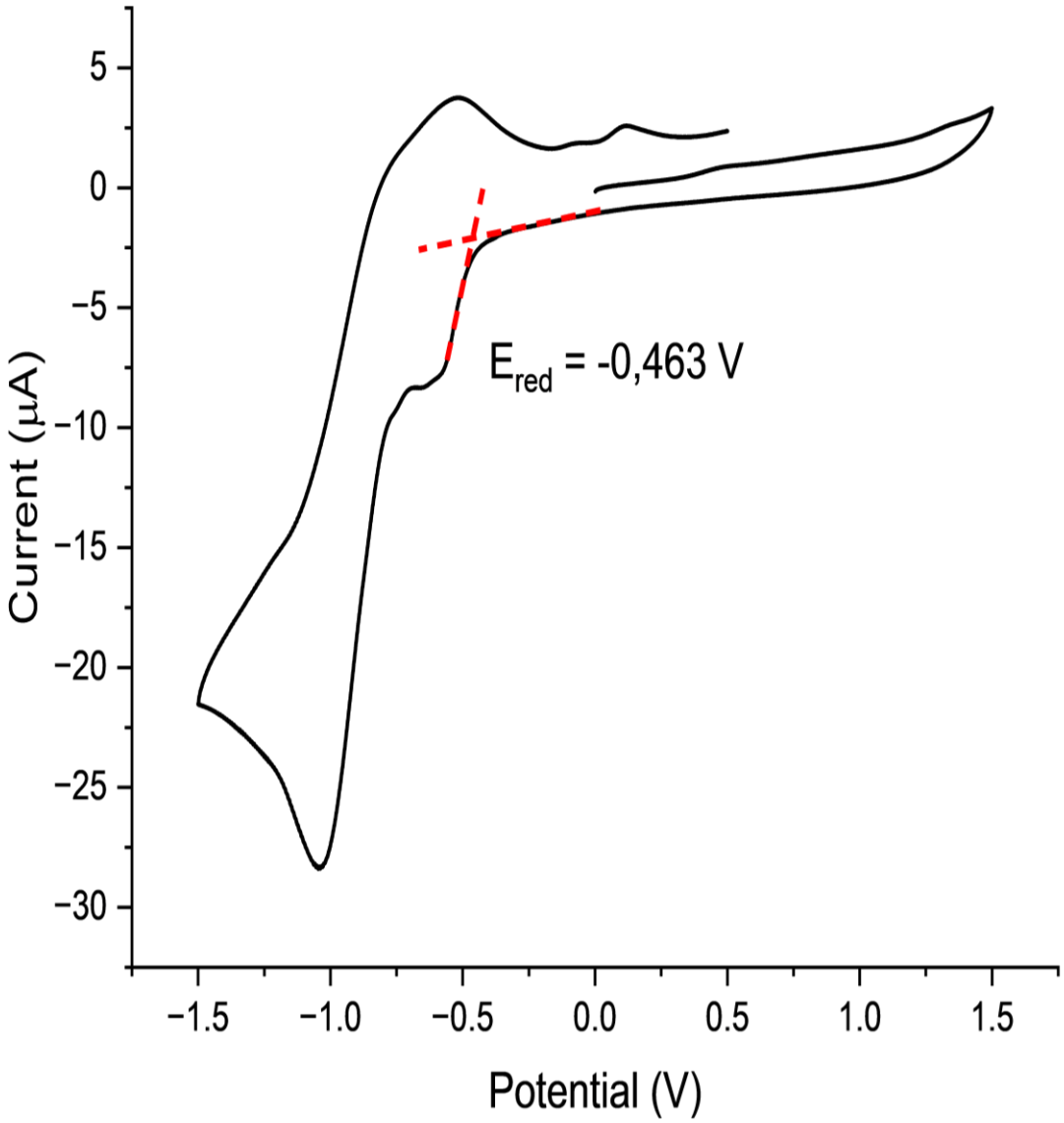



**Figure S10:** Cyclic voltammogram of the photocyclised benzothienoquinolizinium tetrafluoroborate **4** in anhydrous acetonitrile containing 0.1 M $Bu_4NPF_6$, recorded under nitrogen at a scan rate of 50 mV $s^{-1}$. The reduction potential was determined as $E_{red} = -0.463$V vs. Ag/AgCl.

## Computational supporting data

**Table S1.** BSSE-corrected interaction energies calculated for representative FF and FT dimeric π-stacked arrangements of the parent benzothienoquinolizinium (BTQ) scaffold with different $BF_4^-$ counterion positions.

| Dimer arrangement | Counterion position | E(BTQ scaffold monomer) / Hartree | E($BF_4^-$) / Hartree | E(BTQ scaffold dimer) / Hartree | BSSE / Hartree | Interaction energy / kJ $mol^{-1}$ |
|---|---|---|---|---|---|---|
| FF-asym | a | −4931.09707253 | −424.369355413 | −4931.09477383 | 0.06758356 | −203.67 |
| FF-asym | b | −4931.09707253 | −424.369355413 | −4931.07236124 | 0.06372079 | −191.18 |
| FF-asym | c | −4931.09707253 | −424.369355413 | −4931.08905430 | 0.06437849 | −201.67 |
| FF-sym | a | −4931.09707253 | −424.369355413 | −4931.07236744 | 0.06404799 | −191.31 |
| FF-sym | b | −4931.09707253 | −424.369355413 | −4931.09707253 | 0.06573503 | −205.92 |
| FF-sym | c | −4931.09707253 | −424.369355413 | −4931.09679500 | 0.06633785 | −205.17 |
| FF-sym | d | −4931.09707253 | −424.369355413 | −4931.08352468 | 0.06347185 | −197.84 |
| FT-asym | a | −4931.09707253 | −424.369355413 | −4931.09061667 | 0.06586980 | −202.24 |
| FT-asym | b | −4931.09707253 | −424.369355413 | −4931.06406531 | 0.06439794 | −188.53 |
| FT-sym | a | −4931.09707253 | −424.369355413 | −4931.08176840 | 0.06741107 | −197.28 |
| FT-sym | b | −4931.09707253 | −424.369355413 | −4931.06750371 | 0.06403994 | −188.86 |
| FT-sym | c | −4931.09707253 | −424.369355413 | −4931.08006231 | 0.07274929 | −198.03 |

Note: The conformational screening was performed on the parent benzothienoquinolizinium scaffold without the $NO_2$ and CN substituents. The most stabilized FF and FT arrangements identified from the BSSE-corrected interaction-energy screening of the parent BTQ scaffold were used as starting geometries for the nitro/cyano-functionalized FF and FT dimers of compound **4**. After introducing the $NO_2$ and CN substituents, the corresponding dimers were fully reoptimized at the M06-2X/6-311G(d) level.

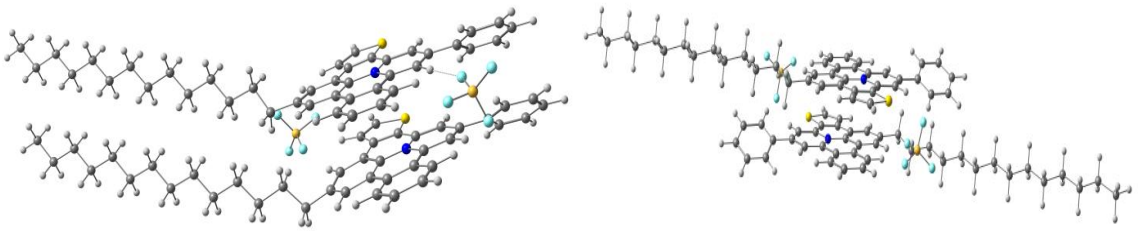


**Figure S11**. Most stable FF and FT π-stacked arrangements selected from the BF4− counterion conformational screening of the parent BTQ scaffold. Left: FF-sym-b; right: FT-asym-a. These geometries were used as starting structures for the nitro/cyano-functionalized dimers of compound **4**.

**Table S2.** Frontier molecular orbital energies calculated using the SMD continuum model for acetonitrile for compound **4** and its π-stacked dimers.

| System | HOMO / eV | LUMO / eV | HOMO–LUMO gap / eV |
|---|---|---|---|
| Monomer **4** | −7.46 | −2.04 | 5.42 |
| Dimer **4**-FF | −7.25 | −2.08 | 5.17 |
| Dimer **4**-FT | −7.00 | −2.00 | 5.00 |

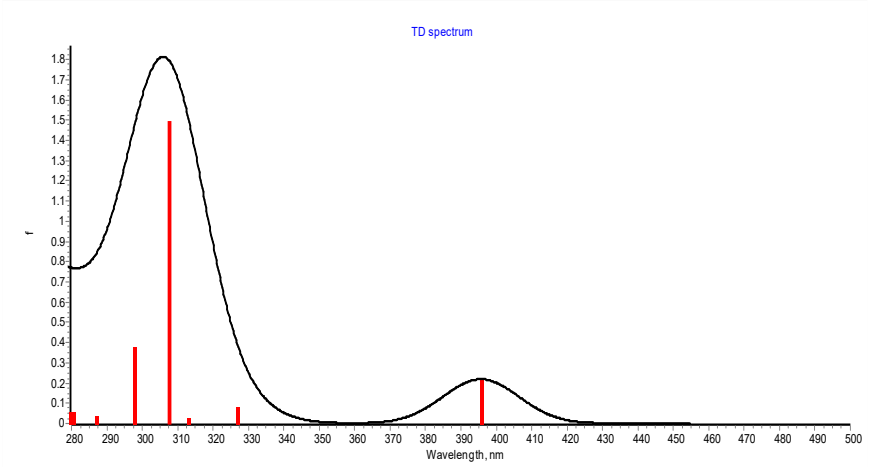



**Figure S12.** Simulated TD-DFT absorption spectrum of compound **4**, calculated at the CAM-B3LYP-D3/6-311G(d)/SMD($CH_3CN$) level on the M06-2X/6-311G(d)-optimized geometry in the gas phase. The red vertical lines represent the calculated electronic transitions and their corresponding oscillator strengths ($f$).

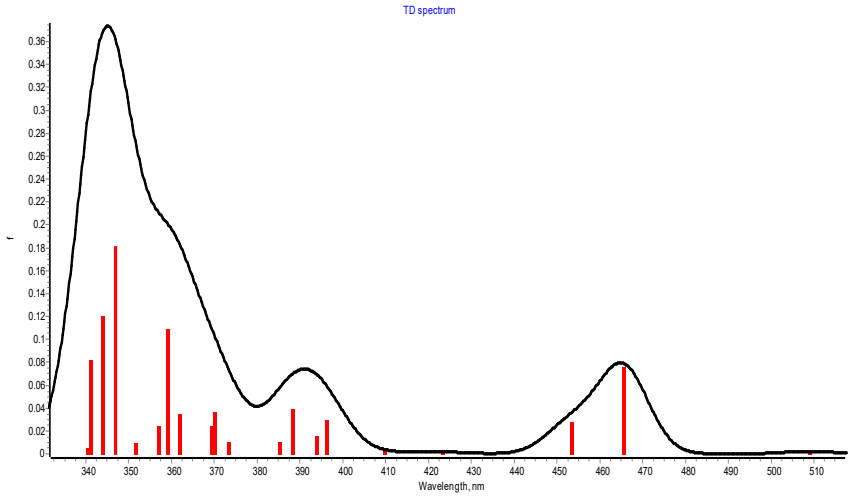



**Figure S13.** Simulated TD-DFT absorption spectrum of the face-to-face (FF) π-stacked dimer of compound **4**, calculated in the gas phase at the B3LYP/6-311G(d) level on the M06-2X/6-311G(d) optimized geometry. The red vertical lines represent the calculated electronic transitions and their corresponding oscillator strengths ($f$).

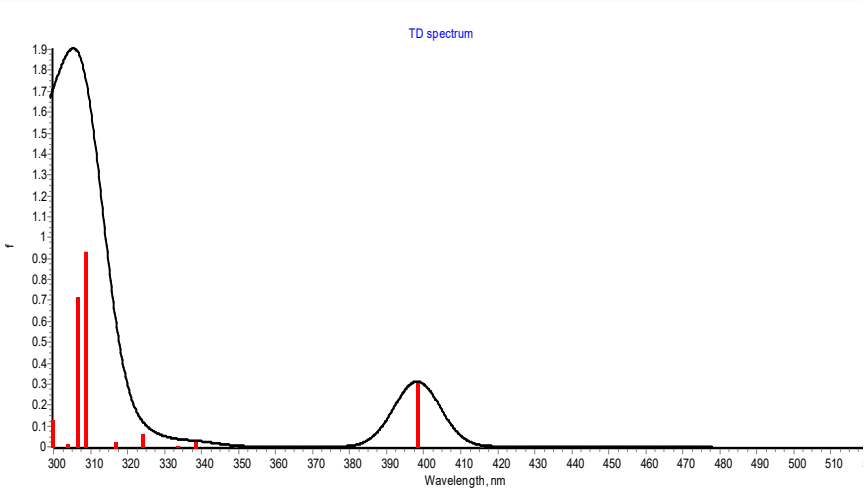



**Figure S14.** Simulated TD-DFT absorption spectrum of the face-to-face (FF) π-stacked dimer of compound **4**, calculated at the CAM-B3LYP-D3/6-311G(d)/SMD($CH_3CN$) level on the M06-2X/6-311G(d) optimized geometry in the gas phase. The red vertical lines represent the calculated electronic transitions and their corresponding oscillator strengths ($f$).

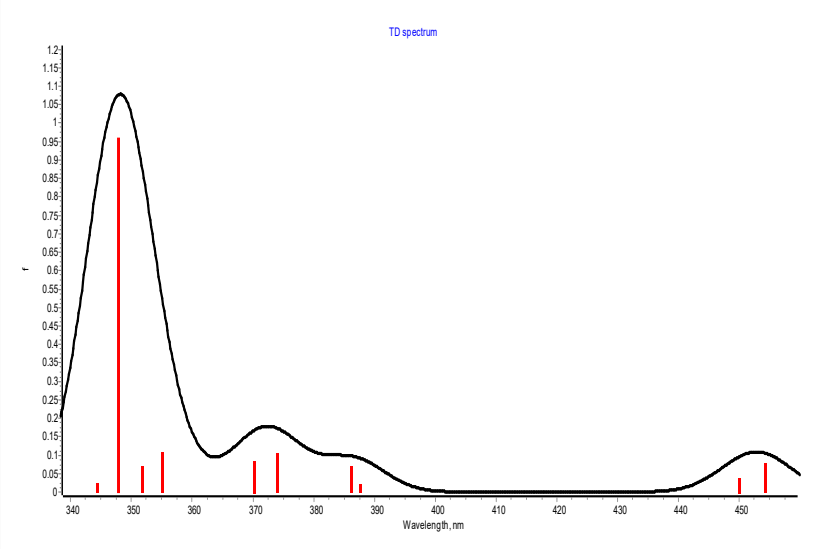



**Figure S15.** Simulated TD-DFT absorption spectrum of the face-to-tail (FT) π-stacked dimer of compound **4**, calculated in the gas phase at the B3LYP/6-311G(d) level on the M06-2X/6-311G(d) optimized geometry. The red vertical lines represent the calculated electronic transitions and their corresponding oscillator strengths (*f*).

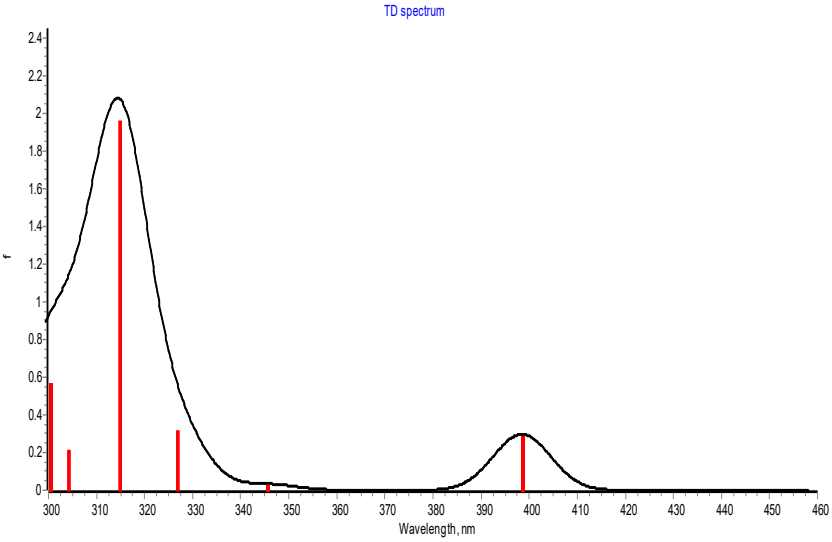



**Figure S16.** Simulated TD-DFT absorption spectrum of the face-to-tail (FT) π-stacked dimer of compound **4**, calculated at the CAM-B3LYP-D3/6-311G(d)/SMD($CH_3CN$) level on the M06-2X/6-311G(d) optimized geometry in the gas phase. The red vertical lines represent the calculated electronic transitions and their corresponding oscillator strengths (*f*).

**Table S3.** Electron excitation descriptors for the selected low-energy transitions of compound **4** and its π-stacked dimers calculated using the SMD continuum model for acetonitrile

| Molecules | Transition | λ / nm | (Δ r / Å) | ($E_{coulomb}$/ eV) | LE / % | CT / % |
|---|---|---|---|---|---|---|
| Monomer 4 | $S_0 \rightarrow S_1$ | 395.7 | 3.70 | 3.48 | 87.3 | 12.7 |
| Dimer 4-FF | $S_0 \rightarrow S_1$ | 415.7 | 3.07 | 2.52 | 50.5 | 49.5 |
| Dimer 4-FF | $S_0 \rightarrow S_2$ | 398.2 | 3.64 | 2.39 | 50.1 | 49.9 |
| Dimer 4-FT | $S_0 \rightarrow S_2$ | 398.5 | 0.020 | 2.65 | 50.0 | 50.0 |

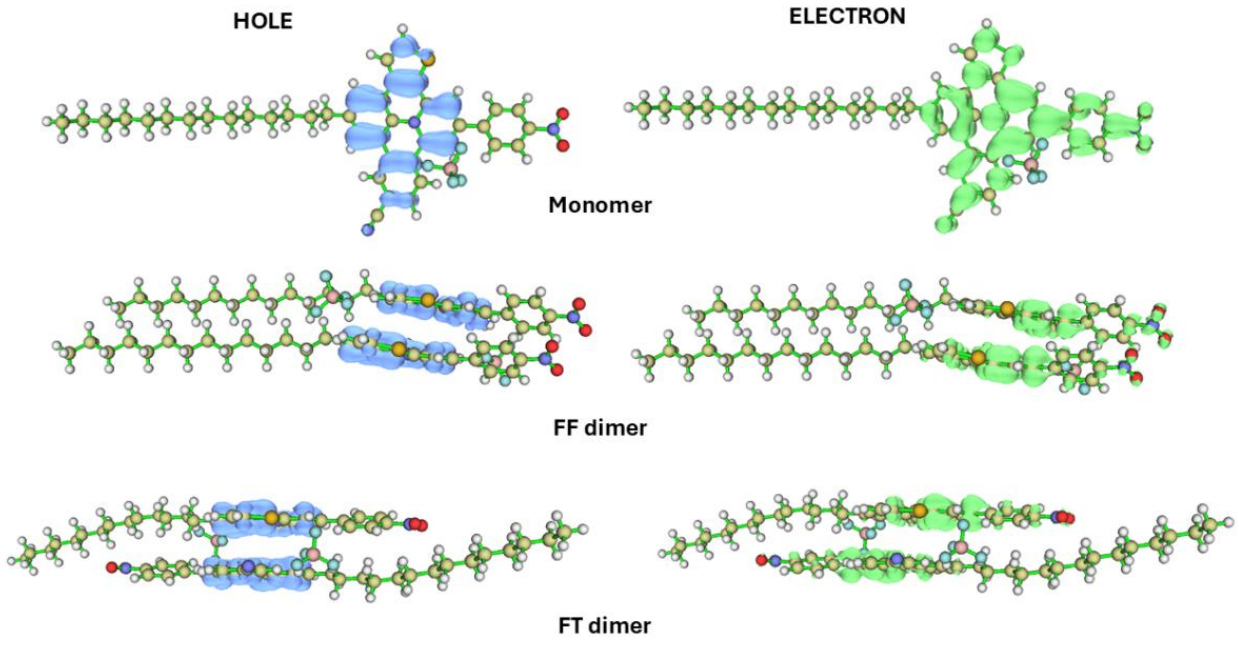



**Figure S17.** Hole (blue) and electron (green) distribution maps for the selected low-energy transitions of compound **4** and its π-stacked dimeric models calculated using the SMD continuum model for acetonitrile.

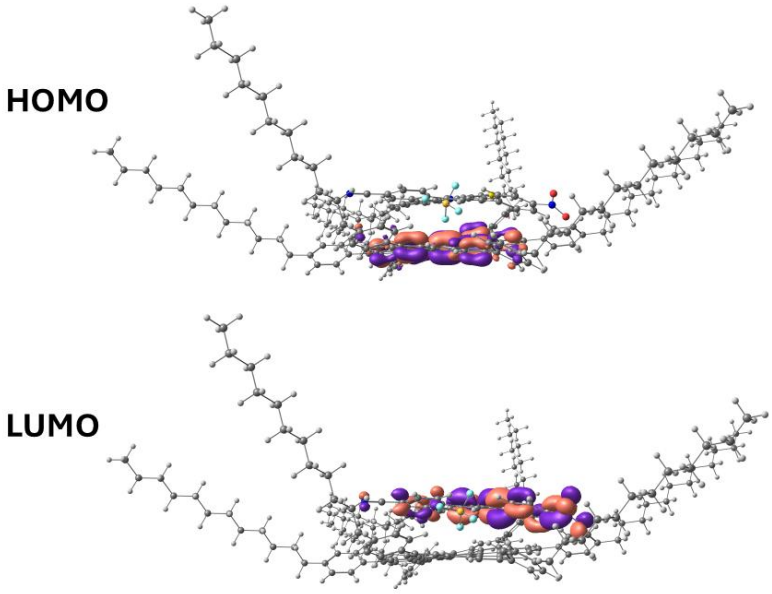



**Figure S18.** Frontier molecular orbital distributions of the HBC-PhC$_{12}$···**4** donor–acceptor complex obtained from single point CAM-B3LYP-D3/6-311G(d)/SMD(CH$_3$CN) calculations on the M06-2X/6-31G(d,p)-optimized geometry in the gas phase.

**Table S4**. Electron excitation descriptors for the selected $S_0 \rightarrow S_1$ transition of the HBC-PhC$_{12}$···**4** donor–acceptor complex calculated using the SMD continuum model for acetonitrile.

| Model | Transition | λ / nm | (Δ r / Å) | ($E_{coulomb}$/ eV) | LE / % | CT / % |
|---|---|---|---|---|---|---|
| HBC-PhC$_{12}$···**4** | $S_0 \rightarrow S_1$ | 437.23 | 5.34 | 2.21 | 3.20 | 96.8 |

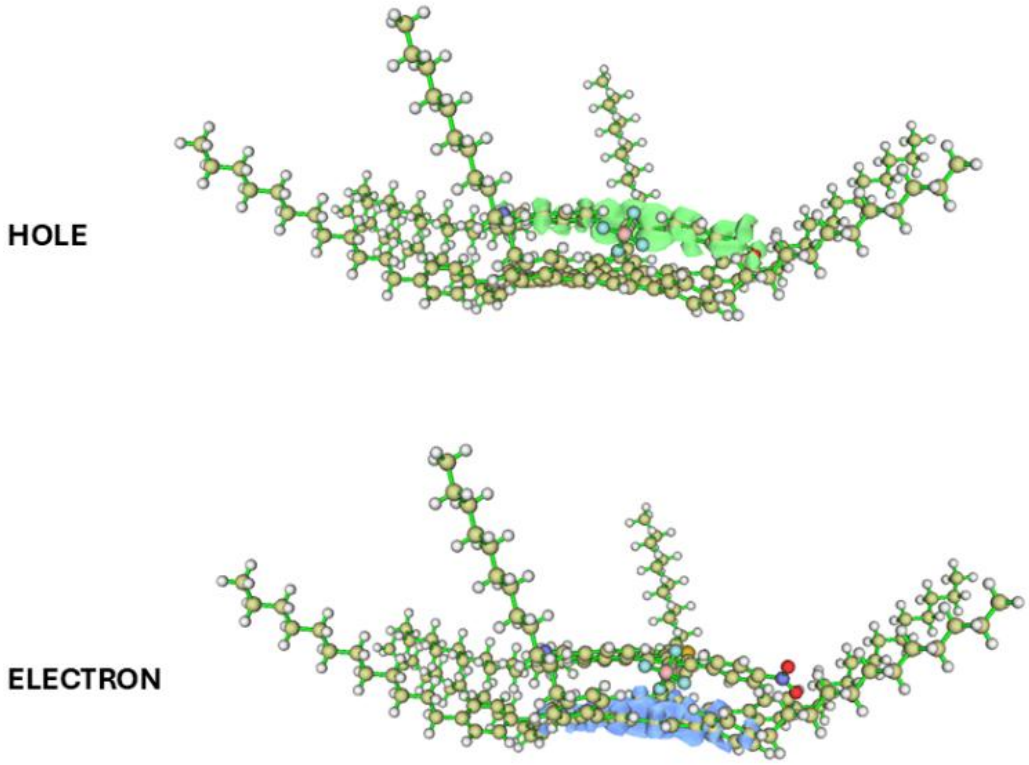



**Figure S19.** Hole and electron distribution maps for the selected HOMO→LUMO transition of the HBC-PhC$_{12}$···**4** complex calculated using the SMD continuum model for acetonitrile. The hole distribution map is shown in blue and the electron distribution map in green.